

## Glassy metallic plastics

LI JianFu, WANG JunQiang, LIU XiaoFeng, ZHAO Kun, ZHANG Bo, BAI HaiYang,  
PAN MingXiang & WANG WeiHua\*

*Institute of Physics, Chinese Academy of Sciences, Beijing 100190, China*

Received December 29, 2009; accepted January 7, 2010

This paper reports a class of bulk metallic glass including Ce-, LaCe-, CaLi-, Yb-, and Sr-based metallic glasses, which are regarded as glassy metallic plastics because they combine some unique properties of both plastics and metallic alloys. These glassy metallic plastics have very low glass transition temperature ( $T_g$ ~25°C to 150°C) and low Young's modulus (~20 GPa to 35 GPa). Similar to glassy plastics, these metallic plastics show excellent plastic-like deformability on macro-, micro- and even nano-scale in their supercooled liquid range and can be processed, such as elongated, compressed, bent, and imprinted at low temperatures, in hot water for instance. Under ambient conditions, they display such metallic properties as high thermal and electric conductivities and excellent mechanical properties and other unique properties. The metallic plastics have potential applications and are also a model system for studying issues in glass physics.

**glassy metallic plastic, synthesizing, low  $T_g$ , thermoplastic, properties**

**PACS:** 81.05.Kf, 81.05.Zx, 64.70.Pf, 62.65.+k, 81.20.Hy

## 1 Introduction

As widely applied materials, polymeric glass and metallic alloy have opposite properties. Polymeric glasses have characteristics of lower glass transition temperature ( $T_g$ ), more stable supercooled liquid region, higher glass-forming ability (GFA) and lower density than those of metal alloys [1,2]. Glassy polymers exhibit excellent thermoplastic molding and imprinting ability as a result of their low  $T_g$ , but with poor mechanical properties, especially in strength. In contrast, metallic alloys exhibit good mechanical properties such as much higher strength and ductility. The metallic glass in particular shows excellent mechanical properties including high elastic strain of ~2% and high compression strength [3], which is much higher than those of their conventional crystalline counterparts. In contrast to polymeric glass, metallic alloys could be cast into desired shapes at a high processing temperature for their high melting

temperature. Different from conventional metallic alloys, most metallic glasses can be processed, such as molding and imprinting, at a lower temperature in their supercooled liquid region, but their  $T_g$  are mostly much higher than that of polymeric glass [4]. Therefore, it is remarkable that a new class of metallic glasses with lower  $T_g$  comparable to polymeric glass can be developed. These alloys would exhibit good thermoplastic behavior like plastics at low temperature and have excellent mechanical and electrical properties under ambient conditions. The combined properties of the alloys make them superior for applications.

Sufficient data on elastic modulus and  $T_g$  of various bulk metallic glasses (BMGs) indicates that there is a clear correlation between Young's modulus and  $T_g$  [5,6]: The lower value of elastic modulus gives lower  $T_g$ . On the other hand, the elastic constants  $M$  of BMGs show a correlation with a weighted average of the elastic constants  $M_i$  for the constituent elements as [5]:  $M^{-1} = \sum f_i \cdot M_i^{-1}$ , where  $f_i$  denotes the atomic percentage of the constituent. The results indicate that the value of  $T_g$  of a BMG depends strongly on

\*Corresponding author (email: whw@aphy.iphy.ac.cn)

the *elastic modulus* of its components. The established correlations between elastic moduli and  $T_g$  provide useful guidelines for the development of glassy metallic plastics with characteristic of low  $T_g$  ( $25^{\circ}\text{C}$ – $200^{\circ}\text{C}$ ). In this letter, we report the formation of a class of glassy metallic plastics including Ce-, LaCe-, CaLi-, Yb- and Sr-based BMGs. The thermodynamic, mechanical and thermoplastic properties of these glassy metallic plastics are investigated.

## 2 Experiment

The Ce- and LaCe- based alloys were prepared by arc-melting pure metals in a Ti-gettered argon atmosphere. The alloy ingots were remelted and suck cast into a Cu mold to get the cylindrical rods or plates. CaLi-, Yb- and Sr-based alloys were prepared by induction melting of mixtures of the pure metals in a quartz crucible in an argon atmosphere and were then cast through a hole into a copper mold to produce cylinder-like samples. The glassy structure of the as-cast alloys was ascertained by X-ray diffraction (XRD) using a MAC M03 XHF diffractometer with Cu K $\alpha$  radiation. The thermal analysis was carried out by a Perkin-Elmer DSC-7 differential scanning calorimeter (DSC) and a Mettler Toledo DSC822e at different heating rates, ranging from 5 to 100 K/min. The acoustic velocities were measured using a pulse echo overlap method by a MATEC 6600 ultrasonic system with a measuring sensitivity of 0.5 ns [7]. The density  $\rho$  was determined by the Archimedean technique and the accuracy lies within 0.1%. Elastic constants (e.g., Young's modulus  $E$ , shear modulus  $G$ , bulk modulus  $K$ , and Poisson's ratio) were derived from the acoustic velocities and the density [7]. The molding or etching samples were investigated by a scanning electron microscope (SEM) to reveal the surface morphology and the fracture features. The electrical resistance of the alloys was measured on a physical property measurement system (PPMS).

## 3 Results and discussion

### 3.1 Design and formation of glassy metallic plastics

According to the modulus criterion, the elements with a low Young's modulus  $E$  ( $< 40$  GPa) are chosen as the base and main components to get the metallic plastics with low  $T_g$ . The first glassy metallic plastic, which is dominated by Ce element ( $E=34$  GPa), was reported in 2005 [8]. Figure 1 shows the DSC curve of the Ce<sub>70</sub>Al<sub>10</sub>Cu<sub>20</sub> glassy metallic plastic. The glass transition in the DSC curve combined with the crystallization exotherm identifies the glassy nature of the Ce-based BMG. The thermodynamic parameters can also be elicited from the DSC trace. The  $T_g$  of the alloy is 341 K, which is much lower than that of the most BMGs [9,10] ( $T_g$  of typical Zr<sub>41</sub>Ti<sub>14</sub>Cu<sub>12.5</sub>Ni<sub>10</sub>Be<sub>22.5</sub> (Vit1) [5] is

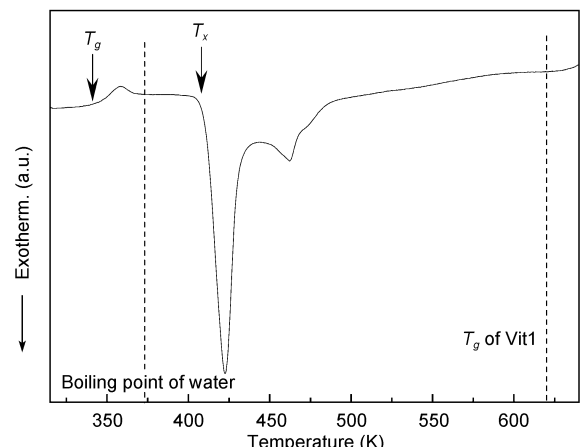


**Figure 1** The DSC curve of as-cast Ce<sub>70</sub>Al<sub>10</sub>Cu<sub>20</sub> BMG at a heating rate of 10 K/min.  $T_g$  of Vit1 and the temperature of boiling water are denoted by the dash lines.

also shown in Figure 1 for comparison) and similar to that of polymeric glass [1] and even lower than the boiling temperature of water. The crystalline temperature ( $T_x$ ) is 408 K which brings on a large supercooled liquid region ( $\Delta T_x = T_x - T_g = 67$  K).

Through modulating the composition, substituting the base or main component, or adulterating a minor element [11], a new series of glassy metallic plastics can be developed. Table 1 lists the various glassy metallic plastics and their thermodynamic parameters. A class of Ce-based BMGs [12] is exploited by modulating the elements of the alloy as shown in Table 1. The Ce<sub>70</sub>Al<sub>10</sub>Cu<sub>20</sub> BMG has the lowest  $T_g$  in those ternary Ce-based BMGs, and the  $T_g$  of all the Ce-based BMGs is in the scale of the polymeric glasses [1]. Furthermore, the  $T_g$  monotonously increases with decreasing Ce ( $E = 34$  GPa) content or with increasing Al ( $E = 70$  GPa) content in Ce<sub>70-x</sub>Al<sub>x</sub>Cu<sub>20</sub> alloys, which is consistent with the modulus criterion [4–6]. In these alloys, Ce<sub>69.5</sub>Al<sub>10</sub>-Cu<sub>20</sub>Co<sub>0.5</sub> BMG has the largest  $\Delta T_x$  (82 K) among the Ce-based alloys, and exhibits a good deformability as a result [9,13]. La element is the neighbor of Ce in the lanthanide series of the periodic table and both have similar atomic radii and moduli. Furthermore, Ce, La or LaCe dominant misch metals are also excellent base elements for preparing the metallic plastics [14–16]. By substituting La partially for Ce in Ce<sub>68</sub>Al<sub>10</sub>Cu<sub>20</sub>Co<sub>2</sub> BMG, a series of LaCe-based glassy metallic plastics, with  $T_g$  ranking from 352 K to 374 K were developed [17] (see Table 1). By introducing Li element (its Young's modulus is 4.9 GPa, which is the lowest in metallic elements) in Ca-based alloy, we exploit a series of CaLi-based glassy metallic plastics with much lower  $T_g$  [18]. The lowest  $T_g$  of CaLi-BMGs is only 35°C, even lower than the human body temperature. Yb- and Sr-based BMGs with the low  $T_g$  close to Ce-based BMGs were also exploited subsequently in 2009 [19,20]. All the BMGs listed in Table 1 are based on the elements with a

**Table 1** The compositions and the thermodynamic parameters including the critical size,  $D$ ,  $T_g$ ,  $T_x$ ,  $\Delta T_x$ , melting temperature  $T_m$ , liquidus temperature  $T_l$ ,  $T_{rg}$ ,  $\gamma$  and  $s$  for the Ce-based, LaCe-based, CaLi-based, Yb- and Sr-based glassy metallic plastics

Composition	$D$ (mm)	$T_g$ (K)	$T_x$ (K)	$\Delta T_x$ (K)	$T_m$ (K)	$T_l$ (K)	$T_{rg}$	$\gamma$	$s$
Ce <sub>70</sub> Al <sub>10</sub> Cu <sub>20</sub>	2	341	408	67	647	722	0.471	0.386	0.18
Ce <sub>70</sub> Al <sub>15</sub> Cu <sub>15</sub>	2	364	406	42	660	686	0.470	0.356	0.13
Ce <sub>65</sub> Al <sub>15</sub> Cu <sub>20</sub>	2	363	425	62	677	773	0.470	0.374	0.15
Ce <sub>60</sub> Al <sub>20</sub> Cu <sub>20</sub>	3	396	444	48	702	830	0.564	0.362	0.11
Ce <sub>55</sub> Al <sub>25</sub> Cu <sub>20</sub>	1	439	479	40	744	825	0.590	0.379	0.10
Ce <sub>69.8</sub> Al <sub>10</sub> Cu <sub>20</sub> Co <sub>0.2</sub>	8	339	414	75	643	721	0.470	0.391	0.20
Ce <sub>69.5</sub> Al <sub>10</sub> Cu <sub>20</sub> Co <sub>0.5</sub>	10	337	419	82	639	716	0.471	0.398	0.22
Ce <sub>69</sub> Al <sub>10</sub> Cu <sub>20</sub> Co <sub>1</sub>	10	340	421	81	634	713	0.477	0.399	0.22
Ce <sub>68</sub> Al <sub>10</sub> Cu <sub>20</sub> Co <sub>2</sub>	10	352	419	67	615	716	0.492	0.392	0.18
Ce <sub>65</sub> Al <sub>10</sub> Cu <sub>20</sub> Co <sub>5</sub>	8	363	414	51	615	695	0.522	0.391	0.15
(Ce <sub>90</sub> La <sub>10</sub> ) <sub>68</sub> Al <sub>10</sub> Cu <sub>20</sub> Co <sub>2</sub>		353	422	69					
(Ce <sub>70</sub> La <sub>30</sub> ) <sub>68</sub> Al <sub>10</sub> Cu <sub>20</sub> Co <sub>2</sub>		358	426	67					
(Ce <sub>50</sub> La <sub>50</sub> ) <sub>68</sub> Al <sub>10</sub> Cu <sub>20</sub> Co <sub>2</sub>		361	419	57					
(Ce <sub>30</sub> La <sub>70</sub> ) <sub>68</sub> Al <sub>10</sub> Cu <sub>20</sub> Co <sub>2</sub>		365	421	55					
(Ce <sub>10</sub> La <sub>90</sub> ) <sub>68</sub> Al <sub>10</sub> Cu <sub>20</sub> Co <sub>2</sub>		365	402	37					
La <sub>68</sub> Al <sub>10</sub> Cu <sub>20</sub> Co <sub>2</sub>		374	439	64					
Ca <sub>65</sub> Li <sub>6.46</sub> Mg <sub>5.54</sub> Zn <sub>23</sub>	2	333	373	40		621	0.536	0.392	0.14
Ca <sub>65</sub> Li <sub>7.54</sub> Mg <sub>6.46</sub> Zn <sub>21</sub>	2	328	360	32		606	0.542	0.385	0.12
Ca <sub>65</sub> Li <sub>8.62</sub> Mg <sub>7.38</sub> Zn <sub>19</sub>	2	327	352	25		597	0.548	0.381	0.09
Ca <sub>65</sub> Li <sub>9.69</sub> Mg <sub>8.31</sub> Zn <sub>17</sub>	3	320	337	17		582	0.550	0.374	0.06
Ca <sub>65</sub> Li <sub>9.96</sub> Mg <sub>8.54</sub> Zn <sub>16.5</sub>	5	317	339	22		581	0.546	0.378	0.08
Ca <sub>65</sub> Li <sub>14.54</sub> Mg <sub>12.46</sub> Zn <sub>8</sub>	2	308	378	70		614	0.502	0.410	0.23
Yb <sub>70</sub> Zn <sub>20</sub> Mg <sub>10</sub>	1	347	386	39	657.5	668	0.519	0.380	0.12
Yb <sub>65</sub> Zn <sub>20</sub> Mg <sub>15</sub>	1	351	393	42	657	676	0.519	0.394	0.13
Yb <sub>62.5</sub> Zn <sub>20</sub> Mg <sub>17.5</sub>	2	367	398	31	629	655	0.560	0.389	0.11
Yb <sub>64</sub> Zn <sub>20</sub> Mg <sub>15</sub> Cu <sub>1</sub>	2	357	402	25	635	722	0.522	0.366	0.07
Yb <sub>69</sub> Zn <sub>20</sub> Mg <sub>10</sub> Cu <sub>1</sub>	2	381	417	36	640	710	0.537	0.382	0.11
Yb <sub>65</sub> Zn <sub>20</sub> Mg <sub>10</sub> Cu <sub>5</sub>	2	384	419	35	641	705	0.545	0.385	0.11
Yb <sub>58</sub> Zn <sub>20</sub> Mg <sub>15</sub> Cu <sub>7</sub>	2	385	415	30	639	720	0.535	0.376	0.09
Yb <sub>62.5</sub> Zn <sub>15</sub> Mg <sub>17.5</sub> Cu <sub>5</sub>	4	381	401	20	638	663	0.575	0.384	0.07
Sr <sub>60</sub> Mg <sub>18</sub> Zn <sub>22</sub>		331	374	43	564	626	0.529		
Sr <sub>60</sub> Li <sub>11</sub> Mg <sub>9</sub> Zn <sub>20</sub>		299	323	24	509	549	0.544		
Sr <sub>60</sub> Mg <sub>20</sub> Zn <sub>15</sub> Cu <sub>5</sub>		335	374	39	566	605	0.554		
Sr <sub>40</sub> Yb <sub>20</sub> Mg <sub>20</sub> Zn <sub>15</sub> Cu <sub>5</sub>		336	378	42	600	637	0.531		

low Young's modulus (Ce: 34 GPa, La: 37 GPa, CaLi: 20 and 4.9 GPa, Yb: 24 GPa) and hence have a quite low  $T_g$  similar to plastics.

According to the classic glass formation criterion, the BMGs with good GFA are identified with  $T_{rg}$  ( $=T_g/T_l$ )  $\geq 0.6$  [10,21], whereas the values of  $T_{rg}$  of the glassy metallic plastics listed in Table 1 are much smaller than 0.6 and even below 0.5. By minor addition of Co element, the GFA of the quaternary Ce-based BMGs can be markedly increased from 2 mm to 1 cm (see Table 1). It is found that the parameters including  $\Delta T_x$ ,  $T_{rg}$ ,  $\gamma$  ( $=\Delta T_x/(T_l + T_g)$ ) [10,21–23] and  $s$  ( $=\Delta T_x/(T_l - T_g)$ ) [24], which are often used to characterize the GFA of the metallic glasses, could not reflect the GFA of these new glassy metallic plastics.

Table 2 shows the density  $\rho$ , the longitudinal acoustic velocity ( $V_l$ ), transversal acoustic velocity ( $V_s$ ),  $E$ , shear modulus ( $G$ ) and bulk modulus ( $K$ ) of the glassy metallic

plastics. All the metallic plastics show the lower  $E$  (below 35 GPa) compared to that of the most BMGs with higher  $T_g$  [5,11].

### 3.2 Plastic-like thermoplastic behavior

The first reported metallic glass, Au-Si metallic glass ribbon [25], has a low  $T_g$  ( $\sim 40^\circ\text{C}$ ) similar to that of the glassy metallic plastics reported in this paper, but it fully crystallizes in 24 hours. Figure 2 shows the temperature-time-transition (TTT) diagrams of Ce<sub>70</sub>Al<sub>10</sub>Cu<sub>20</sub> and Ca<sub>65</sub>Li<sub>9.96</sub>Mg<sub>8.54</sub>Zn<sub>16.5</sub> glassy metallic plastics. According to Arrhenius extrapolation (the dash lines in Figure 2), their predicted lifetimes (the onset time for crystallization) at room temperature (RT:  $25^\circ\text{C}$ ) of Ce<sub>70</sub>Al<sub>10</sub>Cu<sub>20</sub> and Ca<sub>65</sub>Li<sub>9.96</sub>Mg<sub>8.54</sub>Zn<sub>16.5</sub> BMGs are  $\sim 2.6 \times 10^9$  s and  $\sim 7.4 \times 10^6$  s, respectively. Their crystallization incubation times around  $T_g$  derived from Figure 2 are 260 h and 15 h, respectively. The results indicate that the

**Table 2** The elastic constants of the metallic plastics

Composition	$\rho$ (g/cm <sup>3</sup> )	$V_l$ (km/s)	$V_s$ (km/s)	$E$ (GPa)	$G$ (GPa)	$K$ (GPa)
Ce <sub>70</sub> Al <sub>10</sub> Cu <sub>20</sub>	6.699	2.568	1.296	29.91	11.25	29.18
Ce <sub>69.8</sub> Al <sub>10</sub> Cu <sub>20</sub> Co <sub>0.2</sub>	6.733	2.631	1.309	30.82	11.54	31.22
Ce <sub>69.5</sub> Al <sub>10</sub> Cu <sub>20</sub> Co <sub>0.5</sub>	6.744	2.634	1.314	31.08	11.64	31.25
Ce <sub>69</sub> Al <sub>10</sub> Cu <sub>20</sub> Co <sub>1</sub>	6.753	2.628	1.315	31.13	11.68	31.07
Ce <sub>68</sub> Al <sub>10</sub> Cu <sub>20</sub> Co <sub>2</sub>	6.752	2.612	1.322	31.34	11.80	30.33
Ce <sub>68</sub> Al <sub>10</sub> Cu <sub>20</sub> Fe <sub>2</sub>	6.740	2.646	1.316	32.70	12.32	31.35
Ce <sub>68</sub> Al <sub>10</sub> Cu <sub>20</sub> Ni <sub>2</sub>	6.753	2.659	1.332	31.93	11.98	31.77
Ce <sub>68</sub> Al <sub>10</sub> Cu <sub>20</sub> Nb <sub>2</sub>	6.738	2.601	1.315	30.95	11.65	30.06
La <sub>68</sub> Al <sub>10</sub> Cu <sub>20</sub> Co <sub>2</sub>	6.210	2.971	1.391	32.68	12.02	38.77
(Ce <sub>10</sub> La <sub>90</sub> ) <sub>68</sub> Al <sub>10</sub> Cu <sub>20</sub> Co <sub>2</sub>	6.303	2.836	1.332	30.38	11.18	35.77
(Ce <sub>30</sub> La <sub>70</sub> ) <sub>68</sub> Al <sub>10</sub> Cu <sub>20</sub> Co <sub>2</sub>	6.418	2.812	1.345	31.38	11.61	35.29
(Ce <sub>50</sub> La <sub>50</sub> ) <sub>68</sub> Al <sub>10</sub> Cu <sub>20</sub> Co <sub>2</sub>	6.492	2.769	1.337	31.27	11.60	34.32
(Ce <sub>70</sub> La <sub>30</sub> ) <sub>68</sub> Al <sub>10</sub> Cu <sub>20</sub> Co <sub>2</sub>	6.653	2.707	1.335	31.77	11.86	32.93
(Ce <sub>90</sub> La <sub>10</sub> ) <sub>68</sub> Al <sub>10</sub> Cu <sub>20</sub> Co <sub>2</sub>	6.755	2.621	1.306	31.07	11.51	30.75
Ca <sub>65</sub> Li <sub>9.96</sub> Mg <sub>8.54</sub> Zn <sub>16.5</sub>	1.956	4.050	2.139	23.38	8.95	20.15
Ca <sub>65</sub> Li <sub>9.69</sub> Mg <sub>8.31</sub> Zn <sub>17</sub>	1.983	3.915	2.127	23.18	8.98	18.45
Yb <sub>62.5</sub> Zn <sub>15</sub> Mg <sub>17.5</sub> Cu <sub>5</sub>	6.516	2.272	1.263	26.5	10.4	19.8
Sr <sub>60</sub> Mg <sub>18</sub> Zn <sub>22</sub>	3.04	2.862	1.592	19.7	7.71	14.6

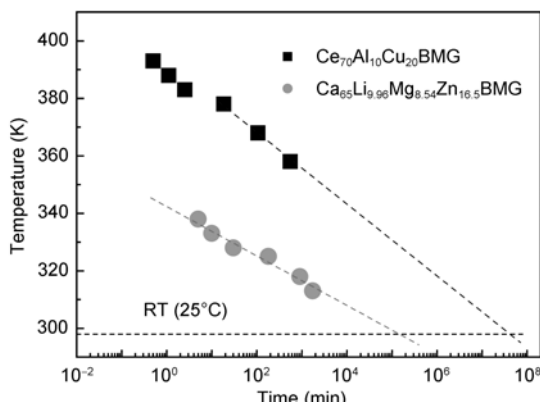


**Figure 2** Time-temperature-transformation (TTT) diagrams for the crystallization incubation of the Ce<sub>70</sub>Al<sub>10</sub>Cu<sub>20</sub> and Ca<sub>65</sub>Li<sub>9.96</sub>Mg<sub>8.54</sub>Zn<sub>16.5</sub> glassy metallic plastics. Isothermal DSC traces [8] and XRD patterns of the iso-thermal crystallized alloy [18] have been used to estimate the crystallization time at a given temperature. The dashed lines are extrapolated at room temperature to show the crystallization incubation time at that temperature.

metallic plastics have good thermal stability in contrast to that of the Au-Si metallic glass at room temperature.

The remarkable feature of the metallic plastics is their plastic-like thermoplastic behaviour. Figure 3(a) shows the true compression stress-strain curves of the Ce<sub>70</sub>Al<sub>10</sub>Cu<sub>20</sub> and Ca<sub>65</sub>Li<sub>9.96</sub>Mg<sub>8.54</sub>Zn<sub>16.5</sub> glassy metallic plastics at RT and in supercooled liquid region. The strengths of the alloys are 490 MPa and 530 MPa, respectively, which are lower in BMGs, such as Zr-based BMGs, but much higher than that of polymeric glass [26]. However, the alloys show polymeric like behaviour when the temperature rises into the supercooled liquid region. The deformation produces a dramatic change in behavior and becomes homogeneous

and shows exceptional plasticity (Figure 3(a)) in the vicinity of  $T_g$ . Above  $T_g$  the alloys can be repeatedly compressed, stretched, bent, and formed into complicated shapes. The inset in Figure 3(a) shows the impression of given patterns of a mold made on the surface of the BMG wafer in hot silicon oil at ~50°C or in hot water demonstrating the excellent thermoplastic processability as the conventional polymeric materials. The final part remains fully glass. A ‘V’ pattern consisting of diamond-shaped microindentation (~30 μm in size) on the surface of the mold using a Vickers hardness tester was replicated in the BMG plate (Figure 3(b) and (c)) indicating the excellent viscous deformability and the possible fabrication of some glassy components in micro- and even in nano-scale [27]. Furthermore, the indents can be erased by annealing [28]. Figure 3(d) shows the clear rectangular strip patterns of a 3 μm width microforming on the surface of Ce<sub>68</sub>Al<sub>10</sub>Cu<sub>20</sub>Co<sub>2</sub> glassy metallic plastics, which forms at about 100°C using silicon die. The exceptional low  $T_g$  and remarkable stability of supercooled liquid state of the materials provide convenient conditions for formability and manufacturability. The molding, shaping and imprinting of the metallic plastics at low temperatures make the apparatus and manufacture process much simpler, cheaper, more convenient, and larger in scale for thermoplastics.

### 3.3 Other unique properties

Besides the low  $T_g$  and the plastic-like thermoplastic behaviour, glassy metallic plastics also have some other unique properties. In general, the transversal acoustic velocity ( $V_s$ ) of the most BMGs exhibits a large change after the crystallization, but the longitudinal acoustic velocity ( $V_l$ )

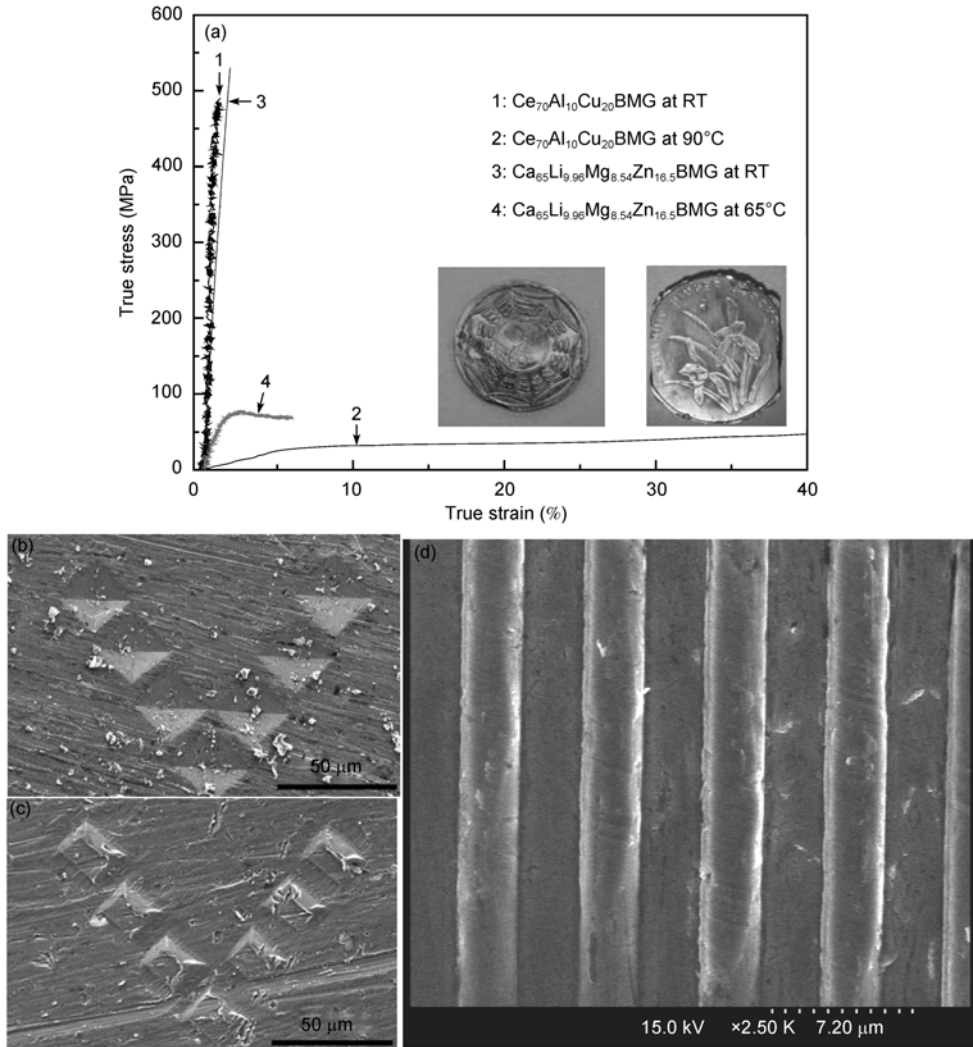


**Figure 3** (a) True stress - true strain curves of a 2 mm-diameter Ce<sub>70</sub>Al<sub>10</sub>Cu<sub>20</sub> (tested under a compression at RT and at 90°C) and Ca<sub>65</sub>Li<sub>9.96</sub>Mg<sub>8.54</sub>Zn<sub>16.5</sub> (tested under a compression at RT and at 65°C (unfractured)). The insets are the Chinese traditional Eight Diagrams (on the surface of Ce<sub>70</sub>Al<sub>10</sub>Cu<sub>20</sub> alloy) and orchid pattern impression (on the surface of the Ca<sub>65</sub>Li<sub>9.96</sub>Mg<sub>8.54</sub>Zn<sub>16.5</sub> alloy) impressed from a mold at one temperature of their supercooled liquid region. (b) SEM pictures of the rectangular strip patterns by microforming on the surface of Ce<sub>68</sub>Al<sub>10</sub>Cu<sub>20</sub>Co<sub>2</sub> metallic plastic using silicon die.

shows no distinct change [29]. However, both the  $V_l$  and  $V_s$  of Ce-based glassy metallic plastics show a dramatic change after crystallization, which means both the longitudinal and transversal acoustic phonons exhibit a soft-mode [30]. Furthermore, the relative change of  $V_l$  and  $V_s$  of Ce-based metallic plastics is negative with the increasing pressure up to 0.5 GPa, which is different from that of other BMGs but similar to the nonmetallic glasses [31]. It is found that there is a covalent bonded short-range ordering structure in the Ce-based glassy metallic plastics. As metallic alloy, the electrical resistivity of the Ce-based glassy metallic plastics is  $\sim 119 \mu\Omega \text{ cm}$  indicating a metallic conductor in contrast to the insulating polymers. The Ce element is characterized by the 4f electrons in the electron structure. In the Ce-based metallic plastics, most of the 4f electrons are local above or below the Fermi level with a relatively small fraction of them being close to the Fermi level. As a result, Ce-based

metallic plastics exhibit heavy-fermion (HF) behavior [32] which differs from that of other metallic glasses [33,34].

Due to the quite low density ( $\rho$ ) and the high compression strength ( $\sigma$ ), CaLi-based glassy metallic plastic exhibits a high specific strength ( $\sigma/\rho$ ) of 271 MPa cm<sup>3</sup> g<sup>-1</sup>, which is similar to that of Zr-based BMGs [35] and higher than that of the conventional crystalline Mg-alloys [36]. Furthermore, CaLi-based BMGs exhibit a good biodegradability. Combined with the low density and low elastic modulus, CaLi-based metallic plastics might have potential application as biomaterials. By using chemical coating method, the corrosion resistance of the CaLi-based alloys can be modulated according to applications of those alloys [37]. Metallic glasses are usually sorted out into strong or fragile glass-forming liquid according to the fragility parameter  $m$  defined by Angell [38]. The  $m$  values of the metallic plastics range from  $20 \pm 3$  to 50 [17–20,39–41]. The

large value range of  $m$  can be used to verify existing correlations in metallic glasses [42]. Metallic plastics also exhibit periodic nanostructures on the fracture surface [43,44] and magnetocaloric effect at low temperature [45–48].

## 4 Conclusions

A series of Ce-, LaCe-, CaLi-, Yb-and Sr-based metallic plastics characterized by low  $T_g$  were developed according to the modulus criterion. These metallic plastics show good GFA, polymer-like thermoplastic behavior at a quite low temperature and some other unique physical and mechanical properties. It is expected that with the development of more metallic plastics with unique physical and chemical properties, the new materials should have great application potentials in data storage and micro- and nano-manufacture.

- 1 Mark J E. Polymer Data Handbook. Oxford: Oxford University Press, 1999
- 2 March N, Tosi M. Polymers, Liquid Crystals and Low-Dimensional Solids. Plenum: New York, 1984. Chap. 1, p.3
- 3 Xi X K, Zhao D Q, Wang W H, et al. Fracture of brittle metallic glasses: Brittleness or plasticity. *Phys Rev Lett*, 2005, 94: 125510
- 4 Wang W H, Dong C, Shek C H. Bulk metallic glasses. *Mater Sci Eng R*, 2004, 44: 45–89
- 5 Wang W H. Correlations between elastic moduli and properties in bulk metallic glasses. *J Appl Phys*, 2006, 99: 093506
- 6 Wang W H. Elastic moduli and behaviors of metallic glasses. *J Non-Cryst Solids*, 2005, 351: 1481–1485
- 7 Wang W H, Wang R J, Zhao D Q, et al. Elastic constants and their pressure dependence of ZrTiCuNiBeC bulk metallic glass. *Appl Phys Lett*, 1999, 74: 1803–1805
- 8 Zhang B, Zhao D Q, Pan M X, et al. Amorphous metallic plastic. *Phys Rev Lett*, 2005, 94: 205502
- 9 Greer A L. Metallic glasses. *Science*, 1995, 267: 1947–1953
- 10 Johnson W L. Bulk glass-forming metallic alloys: Science and technology. *MRS Bull*, 1999, 24: 42–56
- 11 Wang W H. Role of minor additions in formation and properties of bulk metallic glasses. *Prog Mater Sci*, 2007, 52: 540–596
- 12 Zhang B, Wang R J, Zhao D Q, et al. Formation of cerium based bulk metallic glasses. *Acta Mater*, 2006, 54: 3025–3032
- 13 Chen M W. Mechanical behavior of metallic glasses: Microscopic understanding of strength and ductility. *Annu Rev Mater Res*, 2008, 38: 445–469
- 14 Zhang B, Zhao D Q, Pan M X, et al. Metallic plastic based on misch metals. *J Non-Cryst Solids*, 2006, 352: 5687–5690
- 15 Li R, Pang S J, Men H, et al. Formation and mechanical properties of (Ce-La-Pr-Nd)-Co-Al bulk glassy alloys with superior glass-forming ability. *Scr Mater*, 2006, 54: 1123–1126
- 16 Jiang Q K, Zhang G Q, Chen L Y, et al. Centimeter-sized ( $\text{La}_{0.5}\text{Ce}_{0.5}$ )-based bulk metallic glasses. *J Alloys Compd*, 2006, 424: 179–182
- 17 Liu X F, Wang R J, Zhao D Q, et al. Bulk metallic glasses based on binary cerium and lanthanum elements. *Appl Phys Lett*, 2007, 91: 041901
- 18 Li J F, Zhao D Q, Zhang M L, et al. CaLi-based bulk metallic glasses with multiple superior properties. *Appl Phys Lett*, 2008, 93: 171907
- 19 Wang J Q, Wang W H, Bai H Y. Soft ytterbium-based bulk metallic glasses with string liquid characteristic by design. *Appl Phys Lett*, 2009, 94: 041910
- 20 Zhao K, Li J F, Zhao D Q, et al. Degradable Sr-based bulk metallic glass. *Scr Mater*, 2009, 61: 1091–1094
- 21 Turnbull D. Under what conditions can a glass be formed? *Contemp Phys*, 1969, 10: 473–488
- 22 Zhang Y, Zhao D Q, Pan M X, et al. Glass-forming properties of Zr-based bulk metallic glasses. *J Non-cryst Solids*, 2003, 315: 206–210
- 23 Lu Z P, Liu C T. Glass formation criterion for various glass-forming systems. *Phys Rev Lett*, 2003, 92: 115505
- 24 Schroers J. On the formability of bulk metallic glass in its super-cooled liquid state. *Acta Mater*, 2008, 56: 471–478
- 25 Klenment W, Willens R H, Duwez P. Non-crystalline structure in solidified gold-silicon alloys. *Nature*, 1960, 187: 869–870
- 26 <http://www.efunda.com/materials/polymers/properties>
- 27 Kumar G, Tang H X, Schroers J. Nanomoulding with amorphous metals. *Nature*, 2009, 457: 868–872
- 28 Kumar G, Schroers J. Write and erase mechanisms for bulk metallic glass. *Appl Phys Lett*, 2008, 92: 031901
- 29 Okamoto P R, Lam N Q, Rehn L E. Solid State Physics. In: Ehrenreich H, Spaben F, eds. San Diego: Academic Press, 1999, 52: 1–135
- 30 Zhang B, Wang R J, Zhao D Q, et al. Properties of Ce-based bulk metallic glass-forming alloys. *Phys Rev B*, 2004, 70: 224208
- 31 Zhang B, Wang R J, Wang W H. Response of acoustic and elastic properties to pressure and crystallization of Ce-based bulk metallic glass. *Phys Rev B*, 2005, 72: 104205
- 32 Tang M B, Bai H Y, Wang W H, et al. Heavy-fermion behavior in cerium-based metallic glasses. *Phys Rev B*, 2007, 75: 172201
- 33 Tang M B, Bai H Y, Pan M X, et al. Bulk metallic superconductive  $\text{La}_{60}\text{Cu}_{20}\text{Ni}_{10}\text{Al}_{10}$  glass. *J Non-Cryst Solids*, 2005, 351: 2572–2575
- 34 Tang M B, Wang W H. Binary bulk metallic glass. *Chin Phys Lett*, 2004, 21: 901–903
- 35 Gu X, Jiao T, Kecske L J, et al. Crystallization and mechanical behavior of (Hf, Zr)-Ti-Cu-Ni-Al metallic glasses. *J Non-Cryst Solids*, 2003, 317: 112–117
- 36 Neite G, Kubota K, Higashi K, et al. Materials Science and Technology. New York: Wiley, 1996, 8: 152
- 37 Zhao K, Liu K S, Li J F, et al. Superamphiphobic CaLi-based bulk metallic glasses. *Scr Mater*, 2009, 60: 225–227
- 38 Angell C A. Formation of glasses from liquids and biopolymers. *Science*, 1995, 267: 1924–1935
- 39 Zhang B, Pan M X, Zhao D Q, et al. “Soft” bulk metallic glasses based on cerium. *Appl Phys Lett*, 2004, 85: 61–63
- 40 Wei Y X, Zhang B, Wang W H. Erbium and cerium based bulk metallic glasses. *Scr Mater*, 2006, 54: 599–602
- 41 Li S, Wang R J, Pan M X, et al. Formation and properties of  $\text{RE}_{55}\text{Al}_{25}\text{Co}_{20}$  ( $\text{RE} = \text{Y}, \text{Ce}, \text{La}, \text{Pr}, \text{Nd}, \text{Gd}, \text{Tb}, \text{Dy}, \text{Ho}$  and  $\text{Er}$ ) bulk metallic glasses. *J Non-cryst Solids*, 2008, 354: 1080–1088
- 42 Zhao Z F, Zhang Z, Wen P, et al. Highly glass forming alloy with very low glass transition temperature. *Appl Phys Lett*, 2003, 82: 4699–4701
- 43 Wang G, Zhao D Q, Bai H Y, et al. Nanoscale periodic morphologies on fracture surface of brittle metallic glasses. *Phys Rev Lett*, 2007, 98: 235501
- 44 Xia X X, Wang W H, Greer A L. Plastic zone at crack tip: A nanolab for formation and study of metallic glassy nanostructures. *J Mater Res*, 2009, 24: 1–7
- 45 Luo Q, Zhao D Q, Pan M X, et al. Magnetocaloric effect in Gd-based bulk metallic glasses. *Appl Phys Lett*, 2006, 89: 081914
- 46 Wang Y T, Bai H Y, Pan M X, et al. Giant enhancement of magnetocaloric effect in metallic glass matrix composite. *Sci China Ser G-Phys Mech Astron*, 2008, 51: 337–348
- 47 Luo Q, Zhao D Q, Pan M X, et al. Magnetocaloric effect of Ho-, Dy- and Er-based bulk metallic glasses in helium and hydrogen liquefaction temperature range. *Appl Phys Lett*, 2007, 90: 211903
- 48 Wang Y T, Bai H Y, Pan M X, et al. Multiple spin-glass-like behaviors in a Pr-based bulk metallic glass. *Phys Rev B*, 2006, 74: 064422